



THE UNIVERSITY *of* EDINBURGH

Edinburgh Research Explorer

## Heat-induced explosive spalling of self-prestressing, self-compacting concrete slabs

**Citation for published version:**

Mohammed, H, Sultangaliyeva, F, Wyrzykowski, M, Terrasi, G & Bisby, LA 2023, 'Heat-induced explosive spalling of self-prestressing, self-compacting concrete slabs', *Construction and Building Materials*, vol. 372, 130821. <https://doi.org/10.1016/j.conbuildmat.2023.130821>

**Digital Object Identifier (DOI):**

[10.1016/j.conbuildmat.2023.130821](https://doi.org/10.1016/j.conbuildmat.2023.130821)

**Link:**

[Link to publication record in Edinburgh Research Explorer](#)

**Document Version:**

Peer reviewed version

**Published In:**

Construction and Building Materials

**General rights**

Copyright for the publications made accessible via the Edinburgh Research Explorer is retained by the author(s) and / or other copyright owners and it is a condition of accessing these publications that users recognise and abide by the legal requirements associated with these rights.

**Take down policy**

The University of Edinburgh has made every reasonable effort to ensure that Edinburgh Research Explorer content complies with UK legislation. If you believe that the public display of this file breaches copyright please contact [openaccess@ed.ac.uk](mailto:openaccess@ed.ac.uk) providing details, and we will remove access to the work immediately and investigate your claim.



# Heat-induced explosive spalling of self-prestressing, self-compacting concrete slabs

Hussein Mohammed <sup>1,3\*</sup>, Fariza Sultangaliyeva <sup>2</sup>, Mateusz Wyrzykowski <sup>3</sup>, Giovanni Pietro Terrasi <sup>3</sup>,  
Luke Bisby <sup>1</sup>

<sup>1</sup>School of Engineering, The University of Edinburgh, UK

<sup>2</sup>Université de Pau et des Pays de l'Adour, E2S UPPA, SIAME, Anglet, France.

<sup>3</sup>Empa, Swiss Federal Laboratories for Materials Science and Technology, Switzerland.

\*Corresponding author: Hussein Mohammed  
(Hussein.Mohammed@ed.ac.uk)

## Abstract

A novel concrete mix has been developed that can achieve high levels of self-prestressing through the controlled expansion of the concrete sample with cast-in carbon fibre reinforced polymer (CFRP) bars. Experiments have shown that the mechanical properties and durability of the mix are not adversely affected by the mix's self-expanding nature. However, the behaviour of this mix at elevated temperatures is largely unknown, raising legitimate concerns regarding the fire performance of the resulting self-prestressed concrete elements. The research presented in this paper investigates the behaviour of concrete elements manufactured from self-prestressed, self-compacting concrete (SPSCC) when exposed to severe heating – such as would likely be experienced during a building fire. Nine specimens, with dimensions (600 mm × 200 mm × 45 mm) were tested under one-sided exposure to an experimentally simulated ISO 834 standard heating regime. The results showed that the SPSCC samples were acutely prone to explosive spalling under these conditions. The results also suggest that the comparatively higher moisture content of SPSCC samples, as compared with conventional concrete mixes of similar composition and mechanical properties, appeared to be the most critical factor for heat-induced concrete cover spalling. Higher prestress (compressive) forces also appeared to exacerbate the spalling likelihood of SPSCC samples. The addition of 2 kg/m<sup>3</sup> of polypropylene (PP) fibres led to the complete elimination of spalling in SPSCC samples. The self-prestress levels in samples with PP fibres were 30% less than those without PP fibres, for reasons which require additional investigation. Differential thermal expansion between the internal CFRP bars and the concrete was observed to restrain the elongation and thermal curvature of the samples during heating, up until the point where the bars debonded from the surrounding concrete due to elevated temperature and (presumed) increased tensile stress in the tendon anchorage zones. The results provide

38 compelling evidence supporting the need to include PP fibres within high-  
39 performance, self-prestressing, self-compacting concrete slabs.

40

41 **KEYWORDS:** Heat-induced spalling, self-prestressing, CFRP, simulated ISO 834,  
42 Moisture content, Self-compacting concrete

43

44 **Highlights:**

45

- 46 • Production of stable self-prestressed concrete samples.
- 47 • Previously unreported heat induced explosive spalling experiments using a  
48 novel concrete mix.
- 49 • Mitigation of heat induced spalling using PP fibres.

50

51 **Introduction**

52 Prestressed concrete has been widely used in the construction sector for decades.  
53 There are many advantages to prestressed concrete as compared with reinforced  
54 concrete, with the main benefits being a reduction in tension cracking, superior control  
55 of deflections, and more effective utilisation of resources [1]. Prestressed concrete can  
56 be further categorised into pre-tensioned and post-tensioned construction, based on  
57 the manner with which the tensioning of the prestressing bars occurs (i.e., prior to  
58 pouring of the concrete or afterwards). Regardless of the method used, inducing  
59 prestress is a process that requires skilled labour, introduces significant construction  
60 hazards, and is resource heavy; all of which have the potential to make prestressed  
61 concrete less attractive in the construction industry despite its clear functionality and  
62 sustainability benefits.

63 A novel method of achieving comparable prestress levels to those achieved via  
64 traditional methods, and that simplifies casting and prestressing operations, has  
65 recently been developed at Empa [2]. The process uses a concrete mix that experiences  
66 controlled expansion during initial curing, with embedded, bonded, ultra-high  
67 modulus (UHM) carbon fibre reinforced polymer (CFRP) bars (Modulus of Elasticity  
68  $E_{11} = 502$  GPa). Pretension is induced in the CFRP bars in the early stages of curing via  
69 a tailored, controlled expansion of the concrete. Thus, the bulk of the work associated  
70 with pretensioning of the bars, as well as the health and safety hazards associated with  
71 these activities, are eliminated. The self-prestressed, self-compacting concrete  
72 (SPSCC) mix and methodology are reported in detail elsewhere [2], [3].

73 Due to the novelty of this type of self-prestressed concrete mix, research regarding its  
74 behaviour in fire is extremely limited. Preliminary research [4] suggested that SPSCC

75 concrete planks (i.e. thin slabs) are prone to severe heat-induced spalling when  
76 subjected to steep internal thermal gradients (such as generated under exposure to  
77 fire).

78 One of the critically important components of the novel SPSCC mix design is super  
79 absorbent polymer (SAP). SAP particles can absorb several times (more than 15 times)  
80 their mass in moisture during mixing, without becoming dissolved. Therefore, SAP is  
81 used as way to mitigate self-desiccation and autogenous shrinkage for the concrete on  
82 curing by gradually releasing, over time, the moisture that it absorbs during mixing  
83 and casting [5]. However, the water absorbed by the SAP leads to an increased  
84 proportion of effectively free moisture within the concrete. Given the widely accepted  
85 observation that concretes with higher moisture contents are more prone to heat-  
86 induced explosive concrete cover spalling [6], [7], the higher pore moisture content  
87 resulting from SAP addition is likely to affect the spalling propensity of SPSCC mixes.  
88 However, research [8] has also shown the potential positive effects of a combination  
89 of SAP and polypropylene (PP) fibres, when used together, in preventing heat  
90 induced spalling [8]; this was hypothesized as being the result of a higher  
91 interconnectivity of microcracks once the SAP particles are void of water.

92 To explore some of the issues highlighted above, this paper investigates the behaviour  
93 of SPSCC concrete planks under extreme fire loading. The influencing parameters  
94 governing the spalling behaviour of such planks, along with ways to mitigate such  
95 behaviour are considered; this includes the addition of polypropylene fibres (PP),  
96 which have been shown to be very effective in reducing (even eliminating) heat  
97 induced spalling. This paper also considers the effects of drying of samples on the  
98 propensity of concrete planks to spall; and further work is recommended.

## 99 **Methods**

### 100 **Sample Preparation**

101 In total, 9 concrete planks were fabricated using three mixes (three specimens per  
102 mix). Each specimen contained two bars that were made of either UHM CFRP or high  
103 strength steel (see Table 1). The first mix (Ref) was a control mix used as a benchmark.  
104 The second mix (PP) included 2 kg/m<sup>3</sup> of PP microfibres, but otherwise identical to the  
105 control mix. The PP fibres were 18 mm long, and the diameter was 34 µm (on average).  
106 The melting temperature for the PP fibres (as provided by the supplier) was in the  
107 range of 150-170 °C. The third concrete mix (St) was identical to the control mix but  
108 was cast with steel bars instead of CFRP bars. This was done primarily to investigate  
109 the effects of reduced prestressing on spalling, given the lower modulus of elasticity  
110 for the steel bars. The steel bars used had an elastic modulus ( $E_{11}$ ) of 205 GPa,

111 compared to the higher modulus of elasticity for the CFRP bars of 502 GPa. Details of  
 112 the reinforcing bars are given in Table 1.

113 The naming of the samples is based on the mix and the type of internal reinforcement  
 114 used; Ref-CFRP indicates refers to samples made using the Ref mix with CFRP bars,  
 115 Ref-Steel indicates that the samples were made using the Ref mix with steel bars, and  
 116 PP-CFRP means the samples were made using the PP mix and CFRP bars. Letters A,  
 117 B, and C are used to identify the samples in each series.

118 The calcium-sulfoaluminate (CSA), which is the expansive agent, had the following  
 119 composition (determined using Rietveld analysis): anhydrite 48%, ye'elimitite 22%,  
 120 lime 19%, portlandite 9%, periclase 1%, calcite 1%. The Blaine fineness of the CSA  
 121 additive was 0.36 m<sup>2</sup>/g and the density was 2.91 g/cm<sup>3</sup>. The rest of the dry materials  
 122 used for the mix design have been reported fully in previous publications [2], [5], and  
 123 are not repeated here.

124 Table 1 Details of the reinforcing bars used in the current study

Bar Type	Diameter (mm)	E <sub>11</sub>	Remarks
CFRP	5.4	502	Sand-coated
Steel	6.0	205	Ribbed

125

126 The mix composition that was used for each of the 3 batches was identical, except for  
 127 the differences mentioned above. Table 2 provides a detailed mix composition.

128 Table 2 Mix proportion for the concrete casts presented in the current study

Material	Quantity (Reference mix)	Quantity (PP mix)
Cement CEM I 52.5R (kg/m <sup>3</sup> )	491	491
Aggregates (0-8 mm) (kg/m <sup>3</sup> )	1486	1486
SAP (kg/m <sup>3</sup> )	2.76	2.76
Limestone powder (kg/m <sup>3</sup> )	24.6	24.6
Shrinkage reducing agent (RSA) (kg/m <sup>3</sup> )	14.9	14.9
Superplasticiser (% of cement)	1.3%	1.3%
Water (kg/m <sup>3</sup> )	223	223
Calcium-sulfoaluminate cement or CSA cement (kg/m <sup>3</sup> )	78.6	78.6
PP fibres (kg/m <sup>3</sup> )	-	2
Spread (mm)	745	575

129

130 The dry materials were first mixed in a rotating mixer for two minutes. The  
 131 superplasticiser and the SRA were added to the water, which was then added to the  
 132 dry mix. For the second mix (PP), the fibres were added after the addition of the water,  
 133 and mixed for a further two minutes.

134 The fresh concrete was poured into moulds with inner dimensions (200 mm × 600 mm  
 135 × 45 mm). Cylindrical moisture content samples (55 mm high, 55 mm in diameter)  
 136 were also produced to measure the concrete moisture content at the time of fire  
 137 testing. 6 pieces of 160 mm × 40 mm × 40 mm unreinforced concrete prisms were also  
 138 produced to determine the modulus of elasticity and the compressive strength of the  
 139 mixes at 28 and 222 days. The geometry of the samples is shown in Figures 1 and 2.

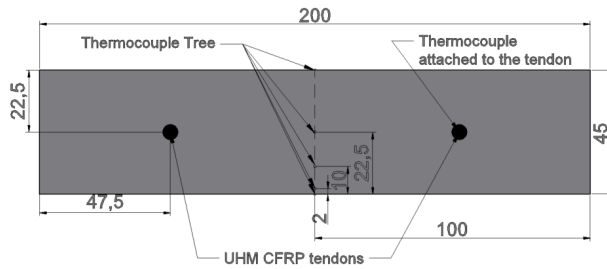


Figure 1 cross section of the planks

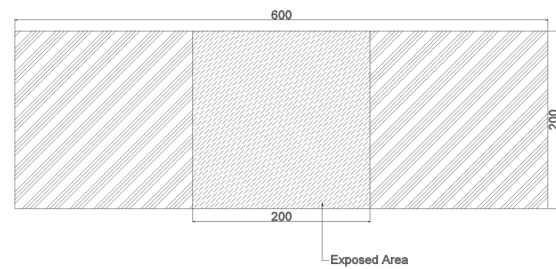


Figure 2 Front elevation view of the samples, with the heated area highlighted

140 A thermocouple (TC) array was inserted into the concrete planks during casting to  
 141 enable in-depth temperature measurement during the spalling experiments (at 2, 10,  
 142 and 22.5 mm from the heat-exposed surface). A further TC was attached to the side of  
 143 one of the prestressing bars at the centre of the concrete plank (i.e., 22.5 mm from the  
 144 heat-exposed surface).

145 During the experiments, two further TCs were used; one was attached to the centre of  
 146 the exposed front of the specimen, and the other to the centre of the unexposed face  
 147 of the sample.

### 148 **Curing**

149 The samples were covered with a polyethylene sheet after casting, and demoulded  
 150 after 20 hours. After demoulding, the samples were transferred to a water bath  
 151 maintained at 20 °C. The samples were removed from the water bath after 28 days and  
 152 transferred to a climate-controlled chamber at 20 °C and 56% relative humidity (RH).  
 153 The samples were removed from the climate chamber after 78 days, and were kept in  
 154 wooden crates, in an uncontrolled laboratory space (at 5-15 °C and 60-70% RH) until  
 155 they were tested. Shipment of the samples from Empa to the University of Edinburgh  
 156 (where the spalling experiments were carried out) took 4 days during the European  
 157 spring season, during which time the environmental conditions were unknown.

### 158 **Prestress development**

159 The development of prestressing in the samples (induced by the presence of UHM  
 160 CFRP bars and the expansion of the concrete) was recorded by resistive linear strain  
 161 gauges (Type HBM SG250, gauge length 6 mm). The strain gauges were bonded to the  
 162 middle of the prestressing bars prior to the casting of the samples. Each sample was

163 equipped with a minimum of two strain gauges (one on each tendon). The bonding of  
164 the strain gauges to the bars is shown in figures 3 and 4. The tendon was first cleaned,  
165 and the strain gauges were bonded to the bars using a fast action glue (HBM Z 70).  
166 The gauges were then covered with three layers of protection to guard against  
167 chemical/mechanical damage during casting and testing. First, a layer of HBM P 140  
168 was used, and after 24 hours a second layer of protective silicon (HBM SG 250) was  
169 added. After a further 7 days, a final layer (HBM AK 22) was applied.

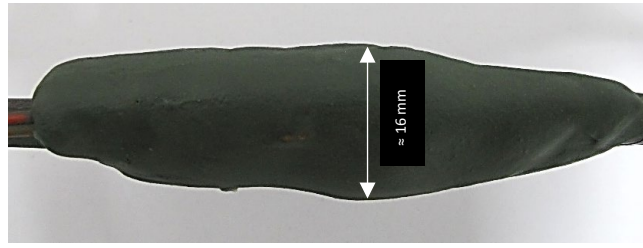
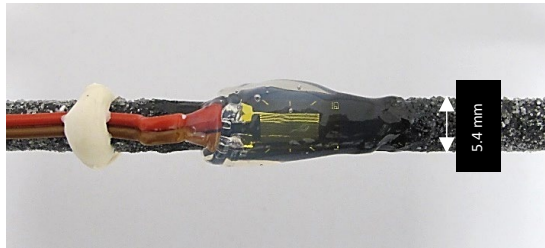


Figure 3 CFRP tendon with HBM SG 250 applied

Figure 4 CFRP tendon with all the protective layers applied

170 Despite the small size of the strain gauges, the protective layers had to be applied over  
171 a relatively large area to ensure adequate protection to the gauges. The resulting,  
172 measured development of prestress (based on strain measurements) with time is  
173 shown in figures 5 through 7.

174 The prestress development within the concrete planks and the variation amongst the  
175 three series of samples is discussed in the self-prestress development section below.

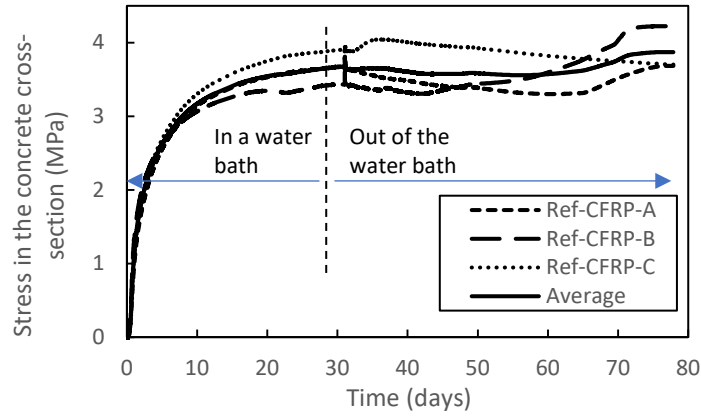


Figure 5 Prestress development in Ref-CFRP samples

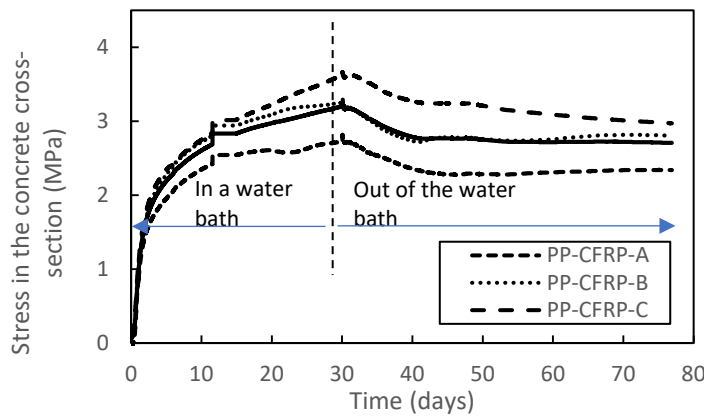


Figure 6 Prestress development in PP-CFRP samples

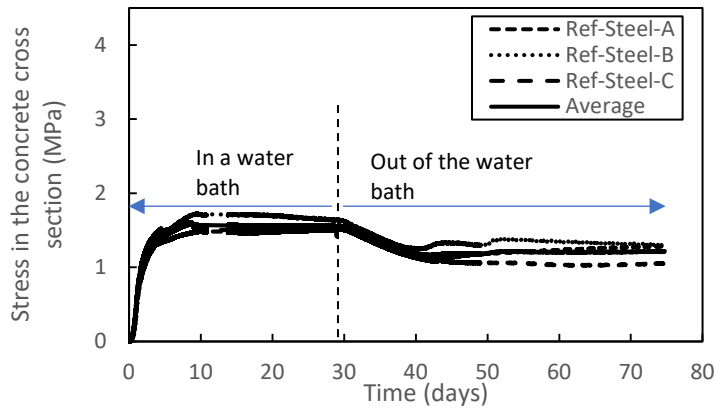


Figure 7 Prestress development in Ref-Steel samples

176

## 177 Mechanical properties at ambient temperature

178 The modulus of elasticity and the compressive strength of the samples were  
 179 determined from tests on small prisms (160 mm × 40 mm × 40 mm) fabricated during  
 180 the casting of the planks. A summary of the mechanical properties for each mix (at  
 181 ambient temperature) is given in Table 3. The values shown in Table 3 are the average,  
 182 and the standard deviation (SD) is given in brackets.



183

184 Table 3 Mechanical properties of the mixes at ambient temperature

Mix	E <sub>11</sub> (MPa) (28 days) (SD)	Compressive strength (MPa) (28 days) (SD)	E <sub>11</sub> (MPa) (180 days) (SD)	Compressive strength (MPa) (222 days) (SD)
Ref	20.5 (0.1)	52.1 (3.75)	28.7 (0.1)	67 (4.28)
PP	21.6 (5.8)	53.6 (3.44)	27.6 (1.8)	65.4 (1.96)
St	20.5 (1.1)	54.9 (2.29)	24.6 (2.8)	60.4 (3.27)

185

### 186 Test set up

187 A mobile, gas-fired radiant panel array (RPA) was used for the spalling experiments.  
188 The working principles of the RPA are reported elsewhere [9]–[11]. The concrete  
189 planks were positioned horizontally (as shown in Figure 2 and 9) and were tested in  
190 a mechanically unrestrained condition (i.e., the samples were free to thermally expand  
191 on heating). The central section of the sample, with a surface area of 200 mm × 200  
192 mm, was exposed to an incident heat flux ( $q''$ ). This was achieved using a 200 mm ×  
193 200 mm opening within a thermally-insulating vermiculite board that shielded the  
194 displacement instrumentation behind. The test set up is shown in Figure 8.

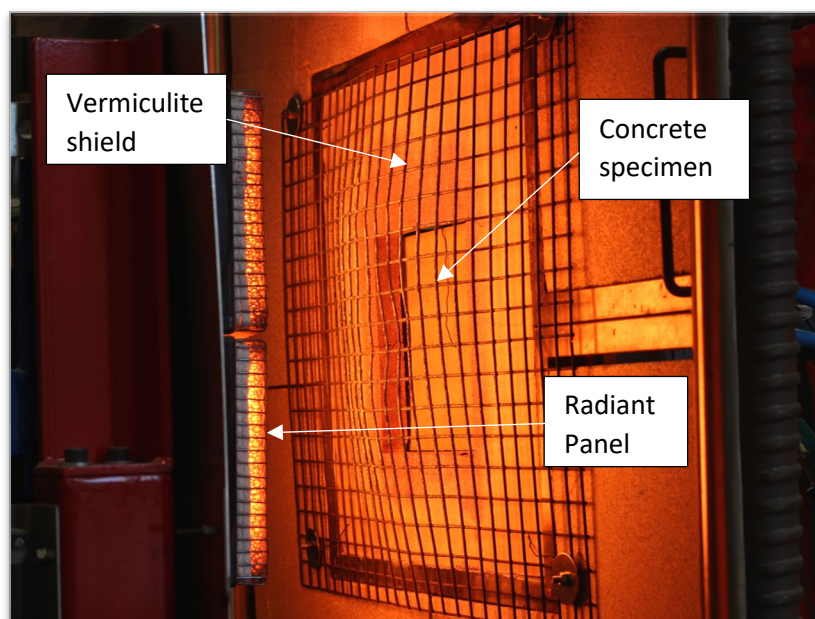


Figure 8 test set up comprising the RPA and the vermiculite shield

195 Thermal bowing of the specimens on heating was measured during the experiments  
196 using three linear potentiometers (LP) that were attached to the cold side of the  
197 specimens (Figure 9). Further LPs were attached to both ends of the specimen (Figure  
198 10) to monitor the elongation of the sample (in-plane) and the draw-in (or slip) of the  
199 prestressing bars upon debonding.

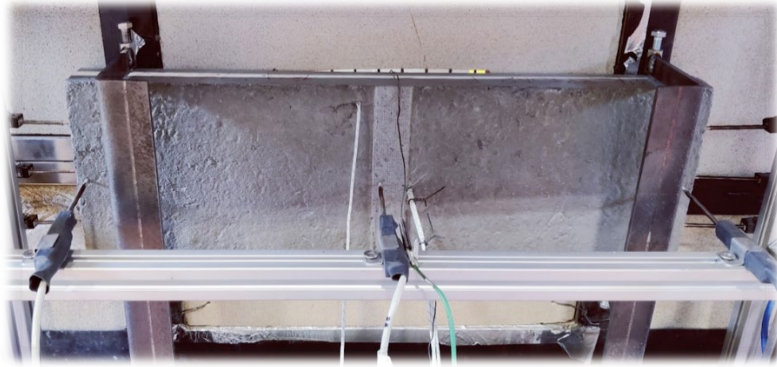


Figure 9 LPs measuring thermal bowing.



Figure 10 LPs measuring elongation.

200 The mobile RPA was used to produce in-depth heating equivalent to that which  
 201 would be experienced under exposure to an ISO 834 standard fire curve. The details  
 202 of the validation of this approach is outlined elsewhere [4], [9].

203 Figure 11 shows a schematic of the out-of-plane curvature (i.e., thermal bowing) of the  
 204 concrete planks when heated.

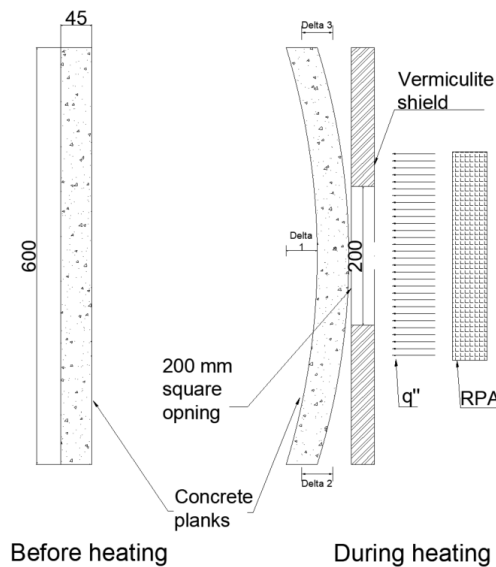


Figure 11 schematic of the thermal bowing (top view) of the horizontally positioned concrete planks.

205 The total magnitude of the thermal bowing (shown in Figure 11 as 'Delta') was  
 206 calculated as the sum of the bowing at the centre of the plank (measured as Delta 1)  
 207 and the average of the reverse movements of the plank at its edges (Delta 2 and Delta  
 208 3).

209 **Testing matrix**

210 The samples were all subjected to the simulated ISO 834 heating exposure for a  
 211 duration of 60 min. However, for the samples that spalled the test was terminated  
 212 after the main spalling event occurred, so as to avoid damaging the RPA. Table 4

213 shows the details of the testing matrix. The moisture content of the samples was  
 214 determined by placing small cylindrical samples in an oven at 105 °C, and measuring  
 215 the weight loss between 24 hour intervals. Drying continued until the difference  
 216 between two consecutive measurements (24 hours apart) was less than 0.1% of the  
 217 dried weight of the sample.

218 Table 4 Mechanical properties and the time-to-spalling for respective samples.

Mix	Type of Bar	Sample	Age (day)	Prestress (MPa)	Test Duration (min)	Tendon slip	Time to spall	Spalling depth (mm)	Moisture content % (at the time of test)
Ref	CFRP	A	150	3.69	9	No	9'00''	12.4	5.93
		B	184	4.22	10	No	5'59''	10.1	5.51
		C	188	3.7	60	Yes	NA	NA	2.46
PP	CFRP	A	192	2.34	60	Partial	NA	NA	5.12
		B	195	2.81	60	No	NA	NA	5.12
		C	196	2.97	60	No	NA	NA	5.12
Ref	Steel	A	190	1.28	15	No	14'56''	23.5	5.51
		B	190	1.3	60	No	NA	NA	5.51
		C	191	1.05	60	No	NA	NA	5.51

219

220 All the samples were aged more than six months when tested, except for Ref-CFRP-  
 221 A, which was five months old at the time of testing. Furthermore, Ref-CFRP-C was air  
 222 dried in an oven (at 80 °C) prior to the experiments. The drying was continued until  
 223 the difference between two consecutive mass measurements (24 hours apart) was less  
 224 than 1% of the sample's mass. This threshold was achieved after 7 days of drying. The  
 225 sample was then left at ambient temperature (in the laboratory where the test took  
 226 place) until the temperature at its centre reached 30 °C (measured with a TC that was  
 227 installed during casting).

## 228 Experimental results

229 The results from the spalling experiments are outlined in Table 4. Both samples Ref-  
 230 CFRP-A and Ref-CFRP-B spalled early. Specimen Ref-CFRP-A experienced one  
 231 instance of violent spalling at 9 minutes and zero seconds (9'00''). specimen Ref-CFRP-  
 232 B first spalled at 5'59'' and continued spalling until 10'00'' when the test was  
 233 terminated. During the experiment on specimen Ref-CFRP-B, 8 instances of spalling,  
 234 of differing severity, were recorded. Figure 8 shows a still-frame image of the  
 235 specimen Ref-CFRP-A at the moment of spalling, and Figure 12 shows specimen Ref-  
 236 CFRP-A after testing. These results are compatible with earlier experiments reported  
 237 in [4]



Figure 12 Still frame of specimen Ref-CFRP-A with debris flying towards the RPA

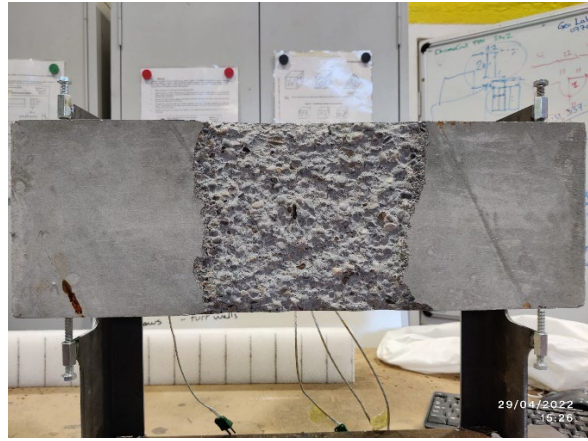


Figure 13 Specimen Ref-CFRP-A after cooling down

238

239 The Ref-CFRP-C specimen (pre-dried at 80 °C for 7 days) did not spall, despite being  
240 subjected to the same heating regime as Ref-CFRP-A and Ref-CFRP-B samples. The  
241 CFRP prestressing bars in specimen Ref-CRFP-C slipped within the concrete at 18'45"  
242 (the temperature at the tendon surface was 250 °C at the moment of slippage). Neither  
243 Ref-CFRP-A nor Ref-CFRP-B samples experienced any tendon slippage.

244 As for the specimens with steel bars (St), Sample Ref-Steel-A experienced one instance  
245 of explosive spalling similar to Sample Ref-CFRP-A. However, Sample Ref-Steel-A  
246 spalled at 14'56" (almost six minutes later than Sample Ref-CFRP-A). The remaining  
247 two specimens belonging to this mix (i.e., samples Ref-Steel-B and Ref-Steel-C) did not  
248 spall. No reinforcement slippage was observed for the specimens with steel bars.

249 Specimens with 2 kg/m<sup>3</sup> of PP fibres completely avoided spalling. In the samples with  
250 PP fibres, the CFRP prestressing bars also avoided slippage. Similar to Ref-CFRP, the  
251 PP-CFRP samples all developed longitudinal reflection cracks (in the concrete along  
252 the lines of the internal prestressing bars) on their unexposed surfaces. However, these  
253 cracks were comparatively less prominent (and narrower) than the cracks observed  
254 for Ref-CFRP-C, and were observed to form at a later stage of heating (see Figure 19  
255 and Table 5).

## 256 Discussion

### 257 Mechanical properties

258 The compressive strengths of the self-prestressed mixes were above 50 MPa and 60  
259 MPa, at 28 days and 222 days, respectively (see Table 3). These strengths were lower  
260 than those reported in similar prior work [2], [3]. The constituent materials used for  
261 the mixes were obtained from the same sources as the mixes reported in these  
262 references, however in the current study the amount of SAP was increased (refer to  
263 Table 2). The cement content for the mixes reported in the current study was also less

264 than in prior work [2], [3]. The inferior strength of the samples in the current work (as  
265 compared to those reported in prior work) can thus be explained by the additional  
266 SAP and the higher water/cement ratio. Previous studies have confirmed that larger  
267 proportions of SAP lead to lower compressive strengths, especially at earlier ages [5].  
268 The results obtained in the current study are thus compatible with prior research.

269 The compressive strength of the specimens tested for this study shows the inadequacy  
270 of the current guidance provided in the Eurocode to mitigate spalling [12]. At present,  
271 spalling mitigation measures (through the addition of PP fibres) are recommended  
272 only when the concrete grade is higher than C80/95. The results from this study show  
273 that the mixes with lower compressive strength than what is outlined in the Eurocode  
274 are still susceptible to explosive spalling, and therefore require spalling mitigation.  
275 Further research has also confirmed the likelihood of low strength concrete to spall  
276 under severe heat conditions [13].

### 277 **Self-prestress development**

278 The time history of self-prestressing for the samples in the current study is shown in  
279 figures 5 through 7. These show that the samples experienced a small amount of  
280 shrinkage once they were taken out of the water bath at 28 days. This is particularly  
281 evident in the Ref-Steel samples and the PP-CFRP samples. The shrinkage continued  
282 for a period of around 10 days before the strain measurements then stabilised.

283 The final measured prestress levels (at 78 days after casting), inferred from strain  
284 gauge readings on the bars, show that self-prestressing in the PP mix was, on average,  
285 30% less than the prestress levels in the Ref mix. The available literature is not  
286 conclusive regarding the effects of PP fibre inclusion on the mechanical properties of  
287 concrete at ambient temperature; wherein some researchers have reported an increase  
288 in the tensile and flexural strength of PP fibre reinforced concrete [14], [15], [16] whilst  
289 others have not observed any measurable difference, or have even reported reductions  
290 in strength with the inclusion of PP fibres [17]. Arguments for the increased tensile  
291 strength are generally based on the idea that PP fibres may prevent the development  
292 of micro-cracks at an early stage of loading. However, once such cracks have formed,  
293 PP fibres (which have a comparatively low modulus) are unlikely to contribute  
294 towards additional strength. During the spalling tests reported herein, it was observed  
295 that specimens with PP fibres developed longitudinal cracks along the CFRP bars at a  
296 later stage of heating than sample Ref-CFRP-C, as shown in Table 5.

297

298

299

300 Table 5 Details of the time-to-cracking and tendon temperature at longitudinal reflective cracking for  
 301 samples with CFRP bars

Reference	PP-CFRP-A	PP-CFRP-B	PP-CFRP-C	Ref-CFRP-C
Time-to-Crack (minutes' seconds''	26'05''	23'47''	32'19''	10'48''
Temperature (°C)	245	224	308	157

302 Table 5 five suggests that the addition of PP fibres may slow down crack propagation,  
 303 which could at least partially explain the reduction in the amount of expansion for  
 304 samples with PP fibres. However, drawing firm conclusions regarding the reason for  
 305 less expansion in the PP mix requires additional research.

306 The levels of prestress would have undoubtedly changed during spalling  
 307 experiments. The changes in the prestress levels are due to the differential thermal  
 308 expansion of the concrete and the CFRP, the deteriorating mechanical and bond  
 309 properties of both the concrete and the prestressing bars embedded within it [18], [19].

### 310 Temperature profiles

311 Figure 14 shows the in-depth temperature-time history for the first 10 minutes of the  
 312 experiments on Ref-CFRP samples. All three samples show comparable in-depth  
 313 temperatures, with the maximum difference being 18 °C in the 10<sup>th</sup> minute. The time  
 314 history of the in-depth temperatures beyond the 10<sup>th</sup> minute are not shown because of  
 315 the occurrence of spalling in samples Ref-CFRP-A and Ref-CFRP-B. No significant  
 316 differences between the time-temperature history for any of the Ref samples was  
 317 evident. Figure 14 demonstrates that the pre-drying of specimen Ref-CFRP-C did not  
 318 lead to obvious variance of heat transfer through the sample when compared against  
 319 specimens Ref-CFRP-A and Ref-CFRP-B.

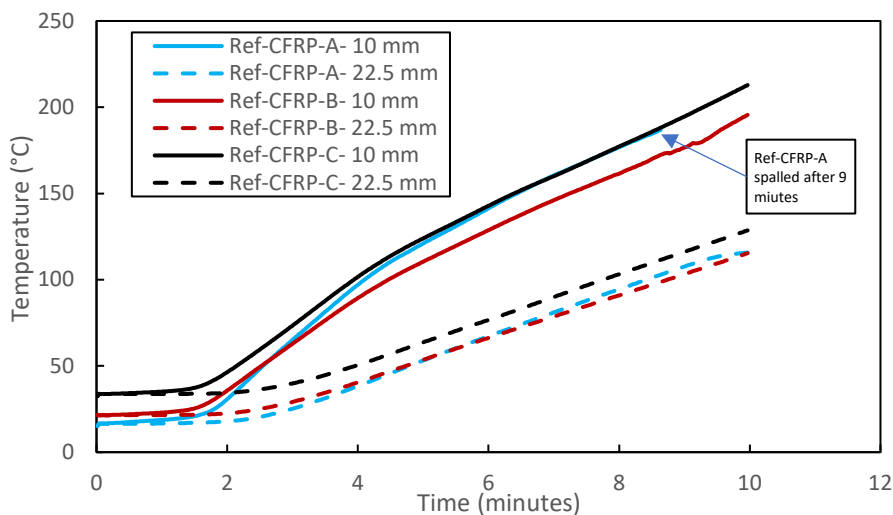


Figure 14 In-depth temperatures (at 10 mm and 22.5 mm) recorded for samples Ref-CFRP-A to Ref-CFRP-C during heating.

320 A comparison of the time-temperature history at the mid depth of the samples  
321 between Ref-CFRP-C and the samples which did not spall is presented in Figure 15.  
322 This figure shows that Sample Ref-CFRP-C (which was pre-dried at 80 °C and thus  
323 also commences at a slightly higher initial temperature) differs from the other samples  
324 in that the temperature evolution at its mid depth fails to show a 'kink' at about 180  
325 °C, thus suggesting that the kink is related to moisture transport and evaporation  
326 within the samples. The kink is thought to be due to the formation of a moving  
327 moisture saturated front (more commonly known as moisture clog).

328 Also evident in Figure 15 is that there is a difference between the PP-CFRP and the  
329 Ref-CFRP samples in terms of the location of the kink. The PP-CFRP samples show a  
330 less acute kink when the temperature reaches about 170 °C. The Ref-Steel samples, on  
331 the other hand, show a more pronounced kink and at a higher temperature (ranging  
332 between 185-195 °C). This could be explained by the enhancement of moisture  
333 migration that occurs when PP fibres are used (i.e., higher rate of moisture migration  
334 into the deeper, colder regions of the heated concrete is made possible when PP fibres  
335 are used). Mcnamee et al. [20] reported observing a much more concentrated wet layer  
336 in samples that contained no PP compared to samples with 1 kg/m<sup>3</sup> of PP fibres (i.e.,  
337 specimens with PP fibres showed evidence of moisture migration further into the  
338 colder regions of concrete compared to specimens without fibres). The more distinct  
339 kinks forming in non-fibre samples (Figure 15) corroborate what was reported by  
340 Mcnamee et. al. [20]. Researchers [21] have also observed that concrete samples with  
341 PP fibres experience rapid increases in gas permeability at temperatures below the  
342 melting point of the fibres; the increased permeability is thought to be explained by  
343 the formation of microcracks in the transition zone within the concrete matrix  
344 surrounding the fibres. The cracks are caused by a thermal mis-match between the  
345 fibres and the concrete [22] which better enables the migration of moisture driven by  
346 temperature gradients.

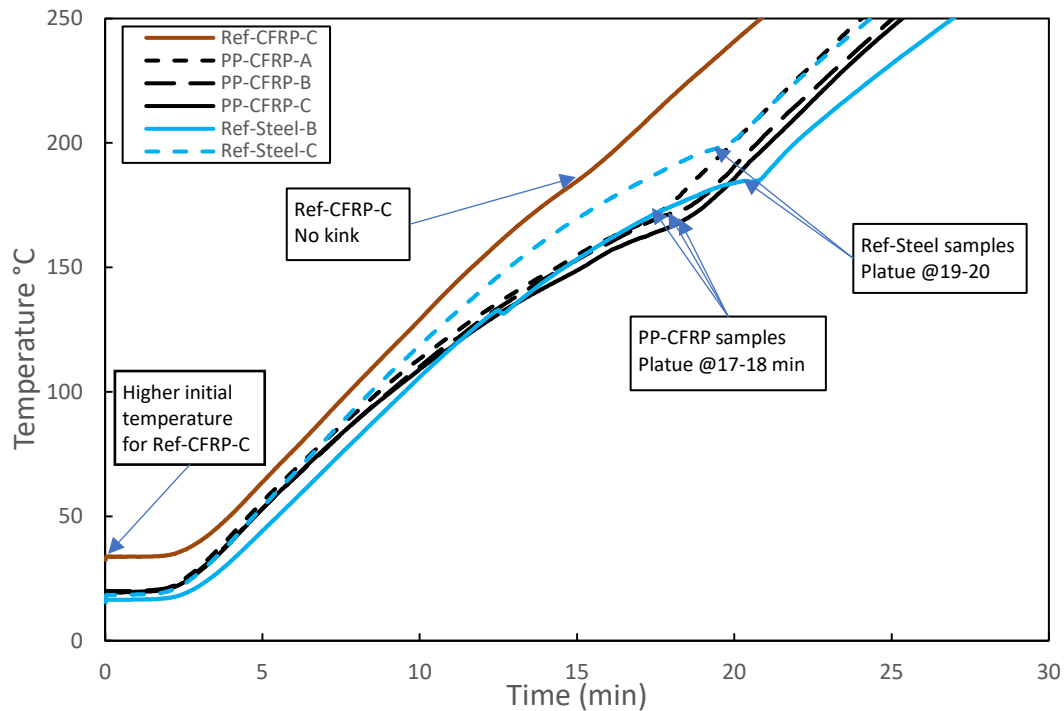


Figure 15 Temperature-time history at the sample mid-depth for the self-prestressed samples that did not experience spalling.

347 Apart from the differences already mentioned, there are no other significant  
 348 differences in the measured in-depth temperatures when comparing Sample Ref-  
 349 CFRP-C and the other samples.

### 350 Thermal Bowing

351 Thermal bowing occurs in the heated plate samples because of differential thermal  
 352 expansion through the specimens' thickness upon rapid heating, and when the  
 353 specimens are mechanically unrestrained. The thermal bowing of both samples Ref-  
 354 CFRP-B and Ref-CFRP-C from the current study is shown in Figure 16. The time  
 355 history of the thermal bowing for Sample Ref-CFRP-B is shown up to the 10<sup>th</sup> minute  
 356 of the experiment (due to subsequent spalling). The thermal bowing of the samples  
 357 appeared – unsurprisingly – to be strongly influenced by the type and behaviour (i.e.,  
 358 slippage or otherwise) of the prestressing bars. Samples with CFRP bars (i.e., Ref-  
 359 CFRP, PP-CFRP) showed greater resistance to overall elongation than samples with  
 360 steel bars (Ref-Steel). This is because the thermal bowing of the Ref-CFRP and PP-  
 361 CFRP samples was restrained by the stiffness of the bars and their slightly negative  
 362 longitudinal coefficient of thermal expansion (CTE) of approximately  $-1.10^{-6}/^{\circ}\text{C}$ .

363 The longitudinal thermal contraction on heating, along with the higher modulus of  
 364 elasticity of the CFRP bars, resists the elongation of the concrete sample – provided  
 365 that bond slippage does not occur. The restraint force ceases to exist, however, once  
 366 the CFRP bars slip within the surrounding concrete matrix. This effect can be clearly



367 seen in Figure 16 (for Ref-CFRP-C sample). By comparison, Figure 17 suggests that the  
368 presence of the steel bars does not have the same restraining effect, and the sample is  
369 more free to thermally expand. This is due to the similarity in the coefficient of thermal  
370 expansion for both concrete and steel, as well as lower modulus of steel bars which  
371 allows a greater overall elongation than for the samples with CFRP bars.

372 Figure 16 shows that the initial bowing (or out-of-plane displacement) for both Ref-  
373 CFRP-B and Ref-CFRP-C are identical (Ref-CFRP-B spalled, Ref-CFRP-C did not  
374 spall). However, the thermal bowing for Ref-CFRP-B deviated from Ref-CFRP-C at  
375 approximately four minutes into the experiment. This was due the higher initial  
376 temperature at the centre of Ref-CFRP-C (30 °C), which led to an increased elongation  
377 (see Figure 15). The thermal bowing of Ref-CFRP-C plateaued after the 10<sup>th</sup> minute  
378 due to the restraint from the CFRP bars mentioned earlier. However, the tendon's  
379 slippage at the 18<sup>th</sup> minute of the experiment (Ref-CFRP-C) led to an increased (and  
380 unrestrained) thermal bowing of the sample (6.42 mm after 60 minutes). This  
381 demonstrates the importance of the internal CFRP reinforcement in restraining  
382 thermal bowing.

383 Figure 17 shows the thermal bowing of Ref-Steel-A and Ref-Steel-C. For Ref-Steel-A,  
384 the results are shown up to the 15<sup>th</sup> minute due to spalling occurring at that time.  
385 Figure 17 shows that there is no obvious difference between Ref-Steel-A and Ref-Steel-  
386 C. Despite this, Ref-Steel-A spalled explosively at 14'56'' while Ref-Steel-C did not  
387 spall. For Ref-Steel-C, the maximum thermal bowing reached at 60 minutes was 6.31  
388 mm (compared with 6.42 mm for CFRP above). No slippage or longitudinal cracks  
389 along the bars were recorded for any of the Ref-Steel samples. This demonstrates that  
390 the steel bars did not have the same restraining effect as the CFRP bars, due to their  
391 coefficient of thermal expansion being similar to concrete – as discussed previously.

392 The results of the thermal bowing for the PP-CFRP samples are shown in Figure 18.  
393 The thermal bowing of specimens with PP fibres is less pronounced as compared with  
394 Ref-Steel samples. This is because the CFRP bars did not slip in this case (except for  
395 one of the two bars in Sample PP-CFRP-A), and thus the restraining effect of the bars  
396 remained in effect, therefore minimizing thermal bowing of all samples with PP fibres.

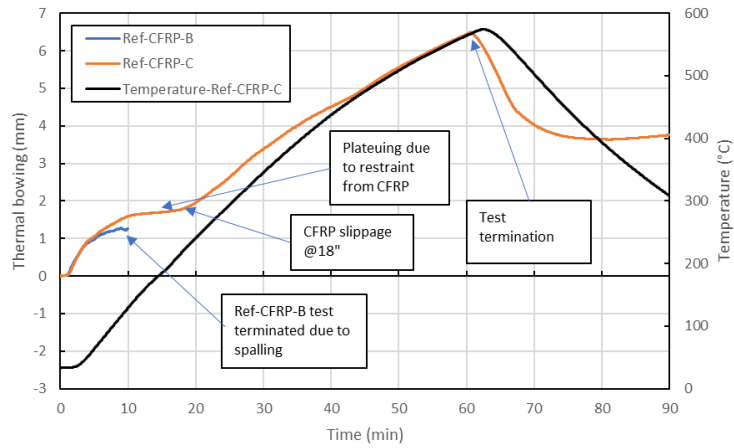


Figure 16 Thermal Bowings Ref-CFRP-B compared to Ref-CFRP-C. The temperature-time history at the centre of the samples is also shown

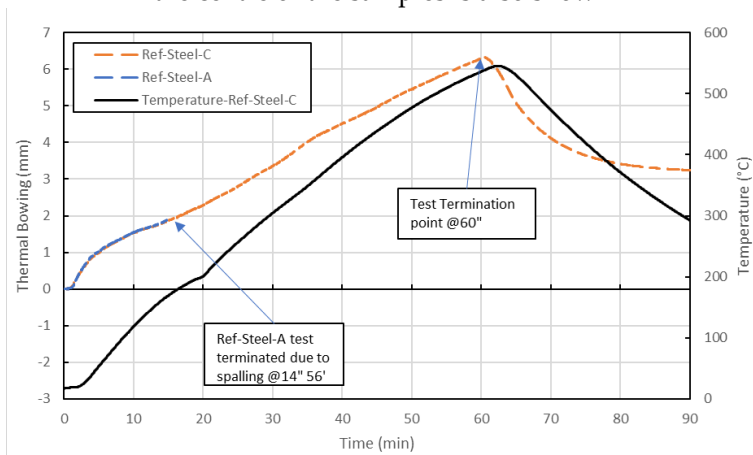


Figure 17 Thermal Bowings Ref-Steel-A compared to Ref-Steel-C. The temperature-time history at the centre of the samples is also shown

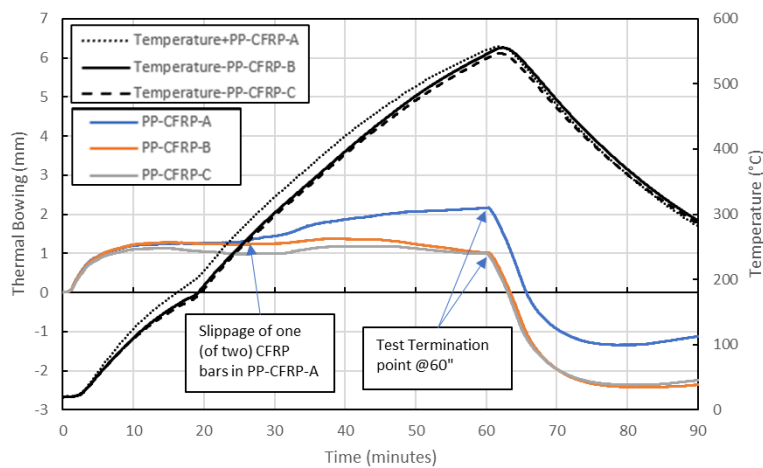


Figure 18 Thermal bowing of PP-CFRP-A, PP-CFRP-B, and PP-CFRP-C samples against time. Temperature at the centre of each sample is shown.

397 The results from the PP-CFRP and Ref-Steel samples provide further evidence that the  
398 restraining of the samples (against thermal bowing) appears not to be a controlling  
399 factor governing the occurrence of spalling.

400 As mentioned earlier, Sample PP-CFRP-A experienced slippage of one of its two bars  
401 at the 24<sup>th</sup> minute of the test. This led to a *partial* release of the restraint imposed by the  
402 CFRP bars. The results of this partial release (i.e., the extra out-of-plane movement)  
403 are visible in Figure 18.

404 A comparison between the thermal bowing of the PP-CFRP samples and Ref-CFRP-B  
405 (up to the 10<sup>th</sup> minute) is shown in Figure 19. This figure shows that the thermal  
406 bowing of Sample Ref-CFRP-B closely matched that of samples with PP fibres, even  
407 though Sample Ref-CFRP-B experienced multiple spalling events from the 6<sup>th</sup> minute  
408 up to the 10<sup>th</sup> minute (the PP-CFRP samples did not spall). This supports the  
409 hypothesis that the thermal bowing (which is a thermal stress release mechanism)  
410 appears not to be a governing factor for the occurrence of spalling; the presence of PP  
411 fibres is the critical factor.

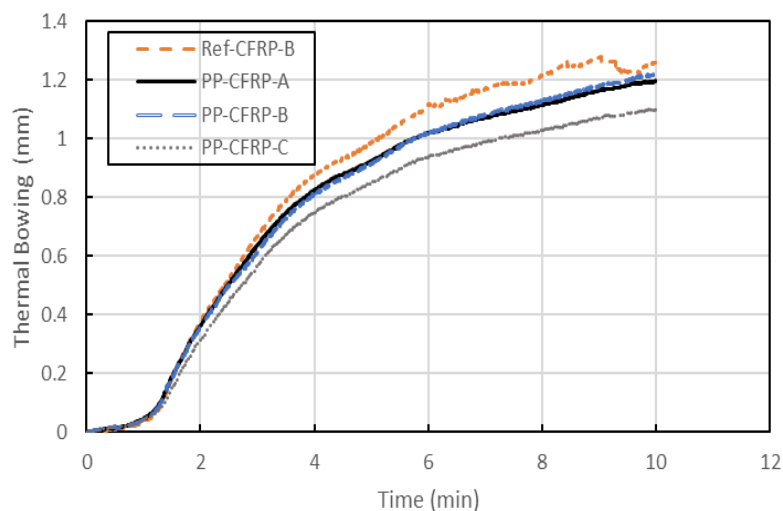


Figure 19 Comparison of thermal bowing between samples Ref-CFRP-B, PP-CFRP-A and PP-CFRP-B.

412

### 413 The Effects of moisture content

414 Moisture content was confirmed to play a central role in spalling. Samples Ref-CFRP-  
415 A and Ref-CFRP-B both spalled explosively, while Sample Ref-CFRP-C did not spall.  
416 All three samples had comparable levels of prestress (see Table 4) and had the same  
417 mix design and internal reinforcement. The only difference between the samples was  
418 the reduced level of moisture within Sample Ref-CFRP-C due to pre-drying. This  
419 result corroborates findings reported by Munguia [23], where concrete slabs exposed  
420 to an ISO 834 fire curve after pre-heating to 80 °C (for more than 30 days) avoided

421 spalling altogether (similar samples that were not dried all spalled). Reduced internal  
422 moisture has been cited by other researchers as one of the main reasons behind  
423 samples avoiding spalling; Peng et al. [24] reported that combined curing led to higher  
424 degree of hydration, and by extension, lower levels of internal moisture. This effect,  
425 according to Peng, resulted in the samples with the lowest amount of internal  
426 moisture (referred to as free moisture by the author) to avoid spalling.

427 The experiments presented in this paper strongly point towards the moisture content  
428 as one of the main influencing factors for spalling. This was evident when comparing  
429 specimen Ref-CFRP-C to Ref-CFRP-B and Ref-CFRP-A. These results are being  
430 confirmed by further experiments.

431 It is noteworthy that some prestress may have been lost in Ref-CFRP-C during the  
432 drying due to shrinkage. This topic is currently being investigated.

### 433 **The effect of prestress levels**

434 The presence of compressive stress is shown in the literature to be (generally)  
435 adversely affecting the spalling likelihood of heated concrete samples [8], [25]. Other  
436 researchers reporting that the direction (relative to crack formation) in which  
437 compressive stress is applied to be the main influencing factor [26] (i.e., when  
438 compressive stress is applied parallel to the cracks, it enhances permeability and  
439 reduces spalling, and vice versa). Nevertheless, the results from Ref-Steel samples  
440 indicate a lower likelihood of spalling with lower prestress levels, since the prestress  
441 in the Ref-Steel samples were on average 69% less than the prestress levels in the Ref-  
442 CFRP samples (due to the lower modulus of elasticity of the steel bars). Further still,  
443 the prestressing within the Ref-Steel samples could have been reduced due to the  
444 deterioration of the elastic modulus of the steel bars with elevated temperatures.  
445 However, the results were not conclusive since one of the three Ref-Steel samples  
446 tested still spalled. Further experiments are needed to verify this hypothesis.

447 As mentioned earlier, it is possible that Ref-CFRP-C (pre-dried) lost some of its  
448 prestress during the drying process (due to shrinkage). It is possible that the potential  
449 reduced levels of prestress levels within this specimen helped it avoid spalling when  
450 subjected to a simulated ISO 834 fire curve. The reduction in prestress levels with oven  
451 drying also needs to be researched further.

452 The samples with PP fibres also had a reduced level of prestress (see Table 4). The  
453 reduced level of prestress could have played a part in the elimination of spalling for  
454 the PP-CFRP samples.

455 Overall, the likelihood of spalling was confirmed to be higher in samples with the  
456 highest levels of prestress. These findings are compatible with has been reported by a  
457 large number of researchers [26]–[30], [31]. It is worth reiterating that compressive  
458 loading on its own may not be a factor that influences spalling; the real effect of  
459 loading is its influence on the further widening or closing cracks that facilitate the  
460 moisture transport, thus increasing or decreasing gas permeability at elevated  
461 temperatures. This effect has been demonstrated experimentally by Jihad et al. [26].

### 462 **Formation of longitudinal cracks**

463 In samples that did not spall, longitudinal splitting cracks were observed to form in  
464 samples with CFRP bars during the experiments. These cracks were not observed in  
465 samples with steel bars. The reason for the longitudinal cracking in CFRP prestressed  
466 samples is likely to be the larger transverse coefficient of thermal expansion (TCTE) of  
467 CFRP bars compared to the surrounding concrete. The temperature in the immediate  
468 surroundings of the CFRP bars at the time of the cracking is given in Table 5. The  
469 TCTE of CFRP is between three to eight times higher than that of concrete and steel,

470 according to Aiello [32]. Some have even reported CTE (in the transverse direction)  
471 8.4 times higher (at 150 °C) than concrete or steel [33]; and also reported the transverse  
472 expansion of the specific CFRP bars used in that work to be temperature dependent  
473 [33], as shown in Figure 20.

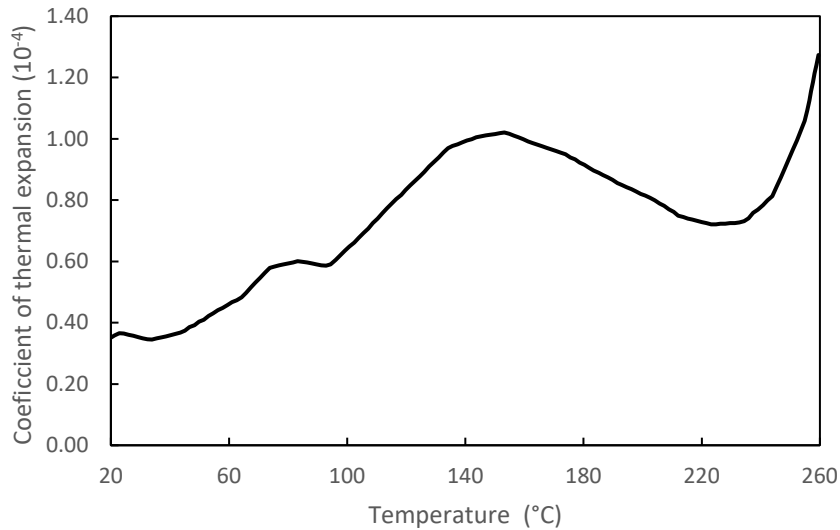


Figure 20 Coefficient of thermal expansion (as a function of temperature) for CFRP bars used and reported in [33]

474 The transverse expansion of the CFRP bars is thought to cause the longitudinal cracks  
475 that were observed during the experiments. Figure 21 shows the unexposed sides of  
476 non-spalled samples Ref-CFRP-C, Ref-Steel-C, and PP-CFRP-C; the longitudinal  
477 cracks can be observed in specimens with CFRP bars, while no cracks are visible in  
478 the specimen with steel reinforcement.

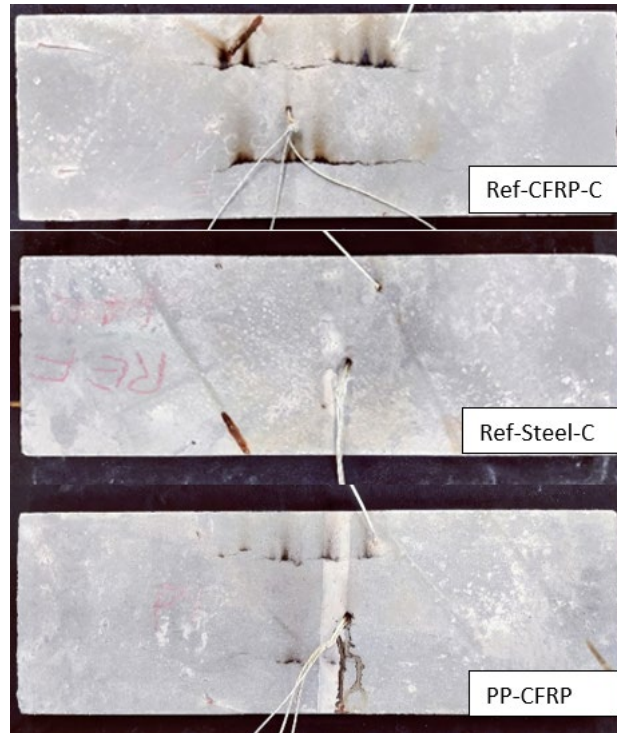


Figure 21 The unexposed side of Ref-CFRP-C (top), Ref-Steel-C (middle), and PP-CFRP-C samples (bottom).

479 It is also noteworthy that longitudinal cracks observed in PP-CFRP samples appeared  
 480 at a later stage than those in sample Ref-CFRP-C (see Table 5). This could be due to  
 481 the effect of the PP fibres slowing down the crack propagation, as has been suggested  
 482 in the literature [15], [16].

### 483 Conclusions

484 The fire behaviour of self-prestressed planks is considered in this paper. Control mixes  
 485 as well as modified mixes (with the addition of PP fibres) were prepared. Using a  
 486 mobile gas-fired RPA, concrete planks were subjected to a simulated ISO 834 heating  
 487 curve for a duration of one hour (or up until a 'main' spalling event). It can be  
 488 concluded that:

- 489 1. Self-prestressed concrete planks are prone to explosive spalling when exposed  
 490 to severe heating (similar to an ISO 834 standard heating exposure). Spalling  
 491 occurred in less than 10 minutes for samples with CFRP bars, but no later than  
 492 15 minutes for any of the samples, when exposed to such conditions.
- 493 2. The higher levels of moisture content in the self-prestressed samples appears  
 494 to be a governing factor for heat-induced spalling. When a specimen was dried  
 495 until it lost more than half of its moisture content (Ref-CFRP-C), no spalling  
 496 was observed, despite other (non-dried) samples within the same series all  
 497 spalling in less than 9 minutes.

- 498 3. The addition of PP fibres to the concrete mix prevented spalling. 2 kg/m<sup>3</sup> of PP  
499 fibres led to the elimination of spalling in samples that were otherwise highly  
500 susceptible to spalling. This corroborates a wealth of available literature  
501 regarding the positive impacts of PP fibres on heat-induced explosive spalling  
502 in concrete.
- 503 4. The addition of PP fibres to the self-prestressed mixes reduced the level of self-  
504 prestressing by almost 30%. Hypotheses have been advanced in this paper to  
505 explain this, but a lack of conclusive evidence means that no firm conclusions  
506 can be made regarding this observation at this stage.
- 507 5. A lower level of prestress appears to reduce the likelihood of spalling. Two out  
508 of three samples with 69% less prestress levels (due to utilising steel bars  
509 instead of CFRP) avoided spalling under otherwise identical heating  
510 conditions.
- 511 6. Thermal stresses appear unlikely to be the governing factor in the spalling of  
512 self-prestressed concrete planks. It was observed that all samples with steel  
513 bars experienced considerable thermal bowing during the tests, but one of three  
514 samples still spalled, whilst very little thermal bowing was recorded for the PP-  
515 CFRP samples, none of which spalled.
- 516 7. In-depth temperature measurements confirm enhanced moisture migration  
517 within the concrete when PP fibres are used. It was observed that the PP-CFRP  
518 samples showed a markedly different in depth thermal response as compared  
519 with samples without PP fibres. This corroborates the role of PP fibres in  
520 facilitating an enhanced rate moisture transport and preventing the formation  
521 of a moisture clog within the concrete, thus mitigating heat-induced explosive  
522 concrete spalling.

### 523 **Future work**

524 Further experiments are necessary to understand the effects of the presence of pre-  
525 compressive stress (from prestressing) on spalling. The role of PP fibres in limiting the  
526 amount of expansion in self-prestressed concrete mixes also requires additional  
527 investigation. Further complimentary tests to thermally characterise the novel  
528 expansive concrete mix are also needed, and will be performed in future work.

### 529 **Acknowledgements**

530 We would like to thank Dr Volha Semianiuk for the help with the initial mix design.  
531 We also acknowledge Mr Sebastiano Valvo, Mr Daniel Völki, Mr Christian Rohrer  
532 (Emma) for their assistance in the laboratory, alongside the efforts of Mark Partington  
533 and Michal Krajcovic from the University of Edinburgh.

534



535 **References**

- 536 [1] C. W. Dolan and H. R. Hamilton, *Prestressed Concrete : Building, Design, and*  
537 *Construction*. 2019.
- 538 [2] M. Wyrzykowski, G. Terrasi, and P. Lura, "Expansive high-performance  
539 concrete for chemical-prestress applications," *Cem. Concr. Res.*, vol. 107, no.  
540 February, pp. 275–283, 2018, doi: 10.1016/j.cemconres.2018.02.018.
- 541 [3] M. Wyrzykowski, G. Terrasi, and P. Lura, "Chemical prestressing of high-  
542 performance concrete reinforced with CFRP tendons," *Compos. Struct.*, vol.  
543 239, no. December 2019, p. 112031, 2020, doi: 10.1016/j.compstruct.2020.112031.
- 544 [4] H. Mohammed, F. Sultangaliyeva, M. Wyrzykowski, G. Pietro Terrasi, and L.  
545 A. Bisby, "An Experimental Study into the Behaviour of Self-Prestressing, Self-  
546 Compacting Concrete at Elevated Temperatures," in *7th International Workshop*  
547 *on Concrete Spalling due to Fire Exposure, 12-14 October 2022*, 2022, pp. 179–193,  
548 [Online]. Available: <https://nbn-resolving.org/urn:nbn:de:kobv:b43-560798>.
- 549 [5] J. Justs, M. Wyrzykowski, D. Bajare, and P. Lura, "Internal curing by  
550 superabsorbent polymers in ultra-high performance concrete," *Cem. Concr.*  
551 *Res.*, vol. 76, pp. 82–90, 2015, doi: 10.1016/j.cemconres.2015.05.005.
- 552 [6] H. Mohammed, H. Ahmed, R. Kurda, R. Alyousef, and A. F. Deifalla, "Heat-  
553 Induced Spalling of Concrete: A Review of the Influencing Factors and Their  
554 Importance to the Phenomenon," *Materials (Basel)*., vol. 15, no. 5, 2022, doi:  
555 10.3390/ma15051693.
- 556 [7] G. Choe, G. Kim, M. Yoon, E. Hwang, J. Nam, and N. Guncunski, "Effect of  
557 moisture migration and water vapor pressure build-up with the heating rate  
558 on concrete spalling type," *Cem. Concr. Res.*, vol. 116, no. October 2018, pp. 1–  
559 10, 2019, doi: 10.1016/j.cemconres.2018.10.021.
- 560 [8] P. Lura and G. Pietro Terrasi, "Reduction of fire spalling in high-performance  
561 concrete by means of superabsorbent polymers and polypropylene fibers:  
562 Small scale fire tests of carbon fiber reinforced plastic-prestressed self-  
563 compacting concrete," *Cem. Concr. Compos.*, vol. 49, pp. 36–42, 2014, doi:  
564 10.1016/j.cemconcomp.2014.02.001.
- 565 [9] C. Maluk, L. Bisby, M. Krajcovic, and J. L. Torero, "A Heat-Transfer Rate  
566 Inducing System (H-TRIS) Test Method," *Fire Saf. J.*, vol. 105, pp. 307–319, 2019,  
567 doi: 10.1016/j.firesaf.2016.05.001.
- 568 [10] I. Rickard, "Explosive Spalling of Concrete in Fire: Novel Experiments under  
569 Controlled Thermal and Mechanical Conditions," p. 390, 2020, [Online].  
570 Available: <https://era.ed.ac.uk/handle/1842/37473>.
- 571 [11] H. Mohammed, D. Morrisset, A. Law, and L. Bisby, "Quantification of the

- 572 thermal environment surrounding radiant panel arrays used in fire  
573 experiments," in *12th Asia-Oceania Symposium on Fire Science and Technology*  
574 (*AOSFST 2021*, 2021, no. December, pp. 7–9, doi: 10.14264/6efaa82.
- 575 [12] "Eurocode 2: Design of concrete structures. General rules - structural fire  
576 design," vol. 1, no. 2005, 2008.
- 577 [13] A. Carlton, Q. Guo, S. Ma, S. E. Quiel, and C. J. Naito, "Experimental  
578 assessment of explosive spalling in normal weight concrete panels under high  
579 intensity thermal exposure," *Fire Saf. J.*, vol. 134, no. August 2021, p. 103677,  
580 2022, doi: 10.1016/j.firesaf.2022.103677.
- 581 [14] H. Mazaheripour, S. Ghanbarpour, S. H. Mirmoradi, and I. Hosseinpour, "The  
582 effect of polypropylene fibers on the properties of fresh and hardened  
583 lightweight self-compacting concrete," *Constr. Build. Mater.*, vol. 25, no. 1, pp.  
584 351–358, 2011, doi: 10.1016/j.conbuildmat.2010.06.018.
- 585 [15] V. Afrouhsabet and T. Ozbakkaloglu, "Mechanical and durability properties  
586 of high-strength concrete containing steel and polypropylene fibers," *Constr.*  
587 *Build. Mater.*, vol. 94, pp. 73–82, 2015, doi: 10.1016/j.conbuildmat.2015.06.051.
- 588 [16] S. Fallah and M. Nematzadeh, "Mechanical properties and durability of high-  
589 strength concrete containing macro-polymeric and polypropylene fibers with  
590 nano-silica and silica fume," *Constr. Build. Mater.*, vol. 132, pp. 170–187, 2017,  
591 doi: 10.1016/j.conbuildmat.2016.11.100.
- 592 [17] A. Sivakumar and M. Santhanam, "Mechanical properties of high strength  
593 concrete reinforced with metallic and non-metallic fibres," *Cem. Concr.*  
594 *Compos.*, vol. 29, no. 8, pp. 603–608, 2007, doi:  
595 10.1016/j.cemconcomp.2007.03.006.
- 596 [18] G. Terrasi, E. R. E. McIntyre, L. A. Bisby, T. D. Lämmlein, and P. Lura,  
597 "Transient thermal tensile behaviour of novel pitch-based ultra-high modulus  
598 CFRP tendons," *Polymers (Basel)*, vol. 8, no. 12, pp. 10–20, 2016, doi:  
599 10.3390/polym8120446.
- 600 [19] Y. N. Chan, X. Luo, and W. Sun, "Compressive strength and pore structure of  
601 high-performance concrete after exposure to high temperature up to 800 °C,"  
602 *Cem. Concr. Res.*, vol. 30, no. 2, pp. 247–251, 2000, doi: 10.1016/S0008-  
603 8846(99)00240-9.
- 604 [20] R. J. Mcnamee, "Fire Spalling – the Moisture Effect," *1st Int. Work. Concr.*  
605 *Spalling due to Fire Expo.*, no. September 2009, 2009.
- 606 [21] J. Bošnjak, J. Ožbolt, and R. Hahn, "Permeability measurement on high  
607 strength concrete without and with polypropylene fibers at elevated  
608 temperatures using a new test setup," *Cem. Concr. Res.*, vol. 53, pp. 104–111,  
609 2013, doi: 10.1016/j.cemconres.2013.06.005.

- 610 [22] D. Zhang, A. Dasari, and K. H. Tan, "On the mechanism of prevention of  
611 explosive spalling in ultra-high performance concrete with polymer fibers,"  
612 *Cem. Concr. Res.*, vol. 113, no. August, pp. 169–177, 2018, doi:  
613 10.1016/j.cemconres.2018.08.012.
- 614 [23] J. C. Mindeguia, P. Pimienta, H. Carré, and C. La Borderie, "Experimental  
615 analysis of concrete spalling due to fire exposure," *Eur. J. Environ. Civ. Eng.*,  
616 vol. 17, no. 6, pp. 453–466, 2013, doi: 10.1080/19648189.2013.786245.
- 617 [24] G. F. Peng, X. J. Niu, Y. J. Shang, D. P. Zhang, X. W. Chen, and H. Ding,  
618 "Combined curing as a novel approach to improve resistance of ultra-high  
619 performance concrete to explosive spalling under high temperature and its  
620 mechanical properties," *Cem. Concr. Res.*, vol. 109, no. March, pp. 147–158,  
621 2018, doi: 10.1016/j.cemconres.2018.04.011.
- 622 [25] C. Maluk, L. Bisby, and G. P. Terrasi, "Effects of polypropylene fibre type and  
623 dose on the propensity for heat-induced concrete spalling," *Eng. Struct.*, vol.  
624 141, pp. 584–595, 2017, doi: 10.1016/j.engstruct.2017.03.058.
- 625 [26] M. J. Miah, H. Kallel, H. Carré, P. Pimienta, and C. La Borderie, "The effect of  
626 compressive loading on the residual gas permeability of concrete," *Constr.*  
627 *Build. Mater.*, vol. 217, pp. 12–19, 2019, doi: 10.1016/j.conbuildmat.2019.05.057.
- 628 [27] R. Jansson and L. Boström, "Factors influencing fire spalling of self compacting  
629 concrete," *Mater. Struct. Constr.*, vol. 46, no. 10, pp. 1683–1694, 2013, doi:  
630 10.1617/s11527-012-0007-z.
- 631 [28] J. Reiners and C. Müller, "Einfluss der Zusammensetzung von Zementstein  
632 auf das Abplatzverhalten von Beton im Brandfall," *Bautechnik*, vol. 95, no. 8,  
633 pp. 547–558, 2018, doi: 10.1002/bate.201800031.
- 634 [29] H. Carré, P. Pimienta, C. La Borderie, F. Pereira, and J. C. Mindeguia, "Effect  
635 of compressive loading on the risk of spalling," *MATEC Web Conf.*, vol. 6, no.  
636 January 2014, 2013, doi: 10.1051/mateconf/20130601007.
- 637 [30] A. Behnood and M. Ghandehari, "Comparison of compressive and splitting  
638 tensile strength of high-strength concrete with and without polypropylene  
639 fibers heated to high temperatures," *Fire Saf. J.*, vol. 44, no. 8, pp. 1015–1022,  
640 2009, doi: 10.1016/j.firesaf.2009.07.001.
- 641 [31] L. Boström, U. Wickström, and B. Adl-Zarrabi, "Effect of specimen size and  
642 loading conditions on spalling of concrete," *Fire Mater.*, vol. 31, no. 3, pp. 173–  
643 186, 2007, doi: 10.1002/fam.931.
- 644 [32] M. A. Aiello, "CONCRETE COVER FAILURE IN FRP REINFORCED BEAMS  
645 UNDER THERMAL LOADING," *J. Compos. Constr.*, vol. 3, no. 1, 1999, doi:  
646 [https://doi.org/10.1061/\(ASCE\)1090-0268\(1999\)3:1\(46\)](https://doi.org/10.1061/(ASCE)1090-0268(1999)3:1(46)).

647 [33] C. Maluk, "Development and Application of a Novel Test Method for  
648 Studying The Fire Baheviour of CFRP Prestressed Concrete Structural  
649 Elements," p. 473, 2014, [Online]. Available: <http://hdl.handle.net/1842/16157>.

650

651